Public Finance Research Papers

ISTITUTO DI ECONOMIA E FINANZA

DIPARTIMENTO DI STUDI GIURIDICI ED ECONOMICI

SAPIENZA UNIVERSITÀ DI ROMA

PUBLIC FINANCE RESEARCH PAPERS

SPATIAL CONVERGENCE IN AGING: THE ROLE OF MIGRATION

ROBERTO BASILE, CINZIA CASTAGNARO, FRANCESCA CENTOFANTI, FRANCESCA LICARI

E-PFRP N. 77

2025

Roberto Basile
Full Professor of Economics
Department of Legal and Economic Studies
Sapienza University of Rome
roberto.basile@uniroma1.it

Cinzia Castagnaro
National Institute of Statistics (ISTAT)
cinzia.castagnaro@istat.it

Francesca Centofanti
University of Rome Tor Vergata
francesca.centofanti@students.uniroma2.eu

Francesca Licari
Italian National Institute of Statistics
francesca.licari@istat.it

Please cite as follows:

Basile R., Castagnaro C., Centofanti F., Licari F. (2025), "Spatial convergence in aging: the role of migration", *Public Finance Research Papers*, Istituto di Economia e Finanza, DSGE. Sapienza University of Rome, n. 77 (https://www.dsge.uniroma1.it/it/ricerca/pubblicazioni/public-finance-research-papers).

E-PFRP N. 77

2025

Spatial Convergence in Aging: The Role of Migration

Roberto Basile[*], Cinzia Castagnaro[†], Francesca Centofanti[‡], and Francesca Licari[§]

Abstract

Population aging challenges welfare systems, particularly in rapidly aging countries such as Italy. Using municipality-level data (2002–2023), this paper examines aging dynamics through the Potential Support Ratio (PSR), the ratio of working-age (15–64) to old-age (65+) population. We apply a beta regression framework to analyze spatial convergence and a two-step decomposition to disentangle the contributions of cohort turnover, mortality, and migration. Findings show strong convergence in aging, with international migration partly mitigating demographic imbalance, while internal migration exacerbates it, increasing fragility in peripheral areas. Policy implications highlight the need to strengthen welfare sustainability and regional equity.

Keywords: Population aging, Migration, Beta convergence, Demographic decomposition, Potential support ratio, Italy.

Jel codes: F22, J61, R23, C14, C21

[*]University of Roma Sapienza, Rome, Italy. Email: roberto.basile@uniroma1.it;

[†]National Institute of Statistics (ISTAT), Rome, Italy. cinzia.castagnaro@istat.it

[‡]University of Rome Tor Vergata, Rome, Italy. francesca.centofanti@students.uniroma2.eu

[§]National Institute of Statistics (ISTAT) and University of Rome Sapienza, Rome, Italy. licari@istat.it; francescamaria.licari@uniroma1.it (Corresponding Author);

Funding: This work was supported by the European Union – *Next Generation EU*" through the PRIN 2022 project titled "Reloading city: a new systemic approach to urban and territorial regeneration" (CUP: E53D23010120006).

1. Introduction

Population aging, driven by rising life expectancy and persistently low fertility, has emerged as one of the most pressing demographic transformations in advanced economies (Bloom & Luca, 2016). On the one hand, socioeconomic progress has extended longevity and reduced mortality (World Health Organization, 2020); on the other, declining fertility has reduced the size of younger cohorts, resulting in a shrinking working-age population. The combination of these forces produces a rising old-age dependency ratio, defined as the share of individuals aged 65 and over relative to the working-age population (15–64). A steadily increasing ratio signals a growing imbalance between retirees and workers, with far-reaching implications for pension systems, welfare sustainability, and economic growth (Bloom et al., 2015; Feldstein, 2006).

The literature has emphasized two main levers to counteract aging. The first is fertility: policies that support families and working mothers can encourage higher birth rates, yet their effects unfold only over the long term, as it takes at least a generation before new cohorts enter the labor force. The second is migration: inflows of younger, economically active individuals can provide a more immediate demographic adjustment, alleviating pressures on the welfare state (Findlay & Wahba, 2013; Neumann, 2013). Migrants are generally younger than the native population, exhibit higher labor force participation, and often have higher fertility rates, thereby both replenishing the workforce and sustaining future population growth (Coleman, 1995; Leers et al., 2004). However, while migration is widely recognized as a potential buffer against aging, the extent to which it can offset the decline in the potential support ratio (PSR) remains debated.

The PSR, defined as the ratio of the working-age population (15–64)[1] to the old-age population (65+), is a widely used indirect measure of aging (UN Population Division, 2000). A lower PSR indicates a greater burden on the active population to sustain retirees, pensions, and healthcare systems. The United Nations "Replacement Migration" report (2000) showed that immigration could partially mitigate the decline in PSR but not fully stabilize it. Later work by Craveiro et al. (2019) confirmed this finding, showing that even with dynamic definitions of working-age and old-age populations, future migration volumes would be insufficient to maintain PSR at current levels.

This demographic challenge is particularly acute in Europe. According to Eurostat (2023), the EU's old-age dependency ratio rose from 27.7% on January 1st, 2013 to 33.4% on January 1st, 2023, with especially high levels in Portugal, Italy, and Finland. Italy represents an extreme case: between January 1st, 2002 and January 1st, 2024, its old-age dependency ratio climbed from 27.9% to 38.3%, making it the country with the largest elderly population in Europe and the second globally after Japan. At the same time, Italy has experienced a reduction in broad regional differences in aging (Basile et al., 2022). In the North, the dependency ratio increased from 29.6% on January 1st, 2002 to 39.2% on January 1st, 2024; in the Center from 30.4% to 39.5%; and in the South (including Sicily and Sardinia) from 24.3% to 36.5% (Istat, 2024). Yet significant spatial heterogeneity persists at finer scales (NUTS-2, NUTS-3, municipalities), reflecting the differentiated impact of demographic drivers across territories. Particularly, Italy's "Inner Areas" have experienced depopulation and youth outmigration, exacerbating demographic fragility (Monturano et al., 2023).

[1] The 15-64 age group is a conventional representation of the working-age population that may not be realistic. Still, it is a standard measure and, therefore, useful in our analysis to assess changes in territories with different demographic and labor supply patterns.

A growing body of research has analyzed spatial convergence in aging in some European countries (Gutiérrez Posada et al., 2018; Backman & Karlsson, 2024), finding evidence of absolute beta-convergence: areas with initially younger populations tend to age faster, reducing regional disparities over time. Other studies have also highlighted how migration interacts with aging across space (Wu et al., 2019; Wu et al., 2021), suggesting that migration plays a crucial role in these dynamics.

Despite these contributions, several gaps remain. First, relatively few studies exploit fine-grained, municipal-level data to capture spatial heterogeneity in aging. Second, the relationship between migration and aging is affected by endogeneity: while migrants are less likely to settle in aging regions, outmigration itself exacerbates aging, making causal interpretations difficult (Prenzel, 2021). Finally, most existing studies emphasize descriptive trends or aggregate forecasts rather than decomposing the demographic drivers of convergence.

To address these gaps, this paper analyzes aging dynamics in Italy using municipality-level data on population stocks and flows (births, deaths, and migration) by age and citizenship between 2002 and 2023. We focus on the Potential Support Ratio (PSR) as our main indicator. First, we apply a beta regression framework to assess spatial convergence in aging, building on approaches by Kashnitsky et al. (2017), Gutiérrez Posada et al. (2018), and Backman & Karlsson (2024). Second, we employ a two-step decomposition method (Kashnitsky et al., 2017) to disentangle the contributions of different demographic components—cohort turnover, mortality, and migration—to changes in PSR. This approach circumvents the endogeneity issues affecting standard econometric models and allows a clearer assessment of migration's role in shaping aging trajectories.

Our analysis is guided by three research questions: *i*) Is Italy experiencing spatial convergence in aging at the municipal level, and to what extent? *ii*) What is the relative contribution of migration, mortality, and cohort turnover to observed changes in the Potential Support Ratio? *iii*) How do international and internal migration differentially shape local demographic trajectories, and what territorial imbalances do they generate?

By answering these questions, the paper advances the literature on demographic transitions, migration, and spatial convergence. We provide new evidence on the mechanisms driving population aging in one of the world's most rapidly aging countries and highlight the territorial implications of demographic change for welfare sustainability and regional development.

The paper is organized as follows: Section 2 outlines the methodology, Section 3 presents descriptive statistics, Section 4 discusses the econometric results, and Section 5 concludes with policy implications.

2. Methodology

2.1. Beta Regression Approach

For each Italian municipality, we calculate the Potential Support Rate (PSR_t) as the ratio between the population aged 15-64 (W_t) and the population aged 65 and over (O_t) at the beginning of each year t (January 1st, year t). To assess convergence in PSR across municipalities, we estimate the following beta regression equation:

$$PSR_t - PSR_{t-1} = \alpha + \beta PSR_{t-1} + \varepsilon_t \quad (1)$$

A negative β parameter indicates absolute convergence in PSR: municipalities with lower PSR values at time $t-1$ tend to catch up with those having higher values, and *vice versa*.[2]

Following Kashnitsky et al. (2017), we decompose the variation in PSR into two steps. First, the change in PSR is separated into an old-age component and a working-age component:

$$PSR_t - PSR_{t-1} = \left[\frac{1}{2}(W_t + W_{t-1})\left(\frac{1}{O_t} - \frac{1}{O_{t-1}}\right)\right] + \left[\frac{1}{2}\left(\frac{1}{O_t} + \frac{1}{O_{t-1}}\right)(W_t - W_{t-1})\right] \quad (2)$$

The second step further decomposes the working-age component - $\left[\frac{1}{2}\left(\frac{1}{O_t} + \frac{1}{O_{t-1}}\right)(W_t - W_{t-1})\right]$ - using the following dynamic equation:

$$W_t = W_{t-1} + CT_{t-1} + M^w_{t-1} - D^w_{t-1} + \Delta^w_{t-1} \quad (3)$$

where $CT_{t-1} = P^{14}_{t-1} - P^{64}_{t-1}$ represents cohort turnover. Here, P^{14}_{t-1} and P^{64}_{t-1} denote the populations aged 14 and 64, respectively, on December 31 of year $t-1$. M^w_{t-1} is the net migration of working-age population between January 1st of year $t-1$ and December 31st of year $t-1$, defined as the balance between inflows and outflows recorded in the municipal registry due to both internal and international migration. D^w_{t-1} is the number of deaths among the working-age population during the same period. Finally, Δ^w_{t-1} is a statistical adjustment for administrative revisions, capturing discrepancies between the population at the beginning and the end of the period (see footnote 7).

Based on equation (3), the working-age component can be decomposed as:

$$\frac{1}{2}\left(\frac{1}{O_t} + \frac{1}{O_{t-1}}\right)(W_t - W_{t-1}) = \left[\frac{1}{2}\left(\frac{1}{O_t} + \frac{1}{O_{t-1}}\right)CT_{t-1}\right]$$

[2] An alternative concept to the β-convergence is the σ-convergence. The latter looks at regional inequalities and analyzes whether the spatial dispersion of the aging (measured by the standard deviation or the coefficient of variation) shrinks or not. A necessary condition for the existence of σ-convergence is the existence of β-convergence (Barro and Sala-i-Martin, 1991).

$$+\left[\frac{1}{2}\left(\frac{1}{O_t}+\frac{1}{O_{t-1}}\right)M_{t-1}^{w}\right]$$

$$-\left[\frac{1}{2}\left(\frac{1}{O_t}+\frac{1}{O_{t-1}}\right)D_{t-1}^{w}\right]$$

$$+\left[\frac{1}{2}\left(\frac{1}{O_t}+\frac{1}{O_{t-1}}\right)\Delta_{t-1}^{w}\right] \quad (4)$$

We then estimate the beta regression separately for each component:

$$\left[\frac{1}{2}(W_t+W_{t-1})\left(\frac{1}{O_t}-\frac{1}{O_{t-1}}\right)\right] = \alpha^{o} + \beta^{o}PSR_{t-1} + \varepsilon_t \quad (5;\ \textit{Old-age})$$

$$\left[\frac{1}{2}\left(\frac{1}{O_t}+\frac{1}{O_{t-1}}\right)(W_t-W_{t-1})\right] = \alpha^{w} + \beta^{w}PSR_{t-1} + \varepsilon_t \quad (6;\ \textit{Working-age})$$

$$\left[\frac{1}{2}\left(\frac{1}{O_t}+\frac{1}{O_{t-1}}\right)CT_{t-1}\right] = \alpha^{ct} + \beta^{ct}PSR_{t-1} + \varepsilon_t \quad (7;\ \textit{Cohort-turnover})$$

$$\left[\frac{1}{2}\left(\frac{1}{O_t}+\frac{1}{O_{t-1}}\right)M_{t-1}^{w}\right] = \alpha^{mg} + \beta^{mg}PSR_{t-1} + \varepsilon_t \quad (8;\ \textit{Migration})$$

$$\left[\frac{1}{2}\left(\frac{1}{O_t}+\frac{1}{O_{t-1}}\right)D_{t-1}^{w}\right] = \alpha^{dt} + \beta^{dt}PSR_{t-1} + \varepsilon_t \quad (9;\ \textit{Deaths})$$

$$\left[\frac{1}{2}\left(\frac{1}{O_t}+\frac{1}{O_{t-1}}\right)\Delta_{t-1}^{w}\right] = \alpha^{\Delta} + \beta^{\Delta}PSR_{t-1} + \varepsilon_t \quad (10;\ \textit{Stat.-Adj.})$$

The overall convergence parameter is given by:

$$\beta \equiv \beta^{o} + \beta^{w} \qquad (11)$$

and, for the working-age component:

$$\beta^{w} \equiv \beta^{ct} + \beta^{mg} + \beta^{dt} + \beta^{\Delta} \qquad (12)$$

A negative β in equation (11) implies convergence in PSR across municipalities. The decomposition further indicates whether convergence is primarily driven by old-age dynamics (β^{o}) or by working-age factors (β^{w}).

It is reasonable to expect a negative sign for the overall β, as evidence from other studies also suggests a gradual but steady catching-up process in aging across regions in Italy. Given the widespread decline in mortality and the rise in life expectancy throughout Italy, a negative β^o is also expected. By contrast, the coefficient for migration (β^{mg}) is likely to be positive, as migration typically generates divergent aging patterns (Smailes et al., 2014; Bloom et al., 2003). For instance, urban areas attract young and often highly educated individuals, thereby rejuvenating local populations, while rural and peripheral areas lose working-age cohorts, accelerating their demographic aging. As argued by Backman and Karlsson (2024), migration thus contributes to greater spatial heterogeneity in age structures.

2.2. Varying-Coefficient Models

A limitation of the previous approach is the assumption of homogeneous β coefficients over time. In this study, we are particularly interested in the time-varying contributions of different components to the overall convergence process. Such heterogeneity can be modeled using semiparametric methods. Specifically, the beta-convergence equation can be reformulated to allow for time-varying coefficients:

$$y_{it} = \alpha + f(t) + f(t)x_{it} + \varepsilon_{it} \quad (13)$$

Here, y_{it} denotes the dependent variable, defined either as the change in PSR ($PSR_{i,t} - PSR_{i,t-1}$) or as one of its components, as described in equations (2) and (4). The regressor x_{it} corresponds to the initial condition ($PSR_{i,t-1}$), while $f(t)$ is a nonparametric smooth function of time estimated using penalized regression splines (details in Appendix 1). By interacting $f(t)$ with the continuous term x_{it}, the model allows the coefficient of x_{it} to vary smoothly over time.

However, equation (13) does not account for observable or unobservable factors that may influence PSR dynamics. An omitted-variable bias could arise if such confounders affect both the dependent and independent variables. Since the regressor x_{it} is predetermined at time $t-1$, simultaneity concerns are mitigated, but issues of reverse causality remain. To reduce endogeneity risks, we refrain from including additional demographic indicators on the right-hand side of equation (13), as they are strongly endogenous.

To capture unobserved spatial and temporal heterogeneity, we extend the model by incorporating a spatiotemporal trend, $g(long_i, lat_i, t)$, defined as a smooth interaction between geographic coordinates and time:

$$y_{it} = \alpha + f(t)x_{it} + g(long_i, lat_i, t) + \varepsilon_{it} \qquad (14)$$

Direct estimation of $g(.)$ can be computationally intensive for large datasets. Therefore, we adopt a spatiotemporal ANOVA decomposition (Lee and Durbán, 2011), which separates the trend into main spatial and temporal effects, as well as their second- and third-order interactions:

$$y_{it} = \alpha + f(t)x_{it} + g_1(long_i) + g_2(lat_i) + g_t(t) + g_{1,t}(long_i, t) + g_{2,t}(lat_i, t) +$$

$$g_{1,2}(long_i, lat_i) + g_{1,2,t}(long_i, lat_i, t) + \epsilon_{it}$$

The model is estimated via penalized regression, combining basis representations of the unknown functions with smoothness penalties. We use the cubic B-spline method introduced by Eilers and Marx (1996), which applies second-order differences of adjacent coefficients as penalties (see Appendix 1 for technical details).[3]

[3] We use the gam() function included in the mgcv R package to estimate the model.

3. Spatial Distribution of Aging in Italy

This section reports the results of the analysis of the spatial distribution of aging in Italy over the period 2002–2023. Aging is measured using the Potential Support Ratio (PSR), calculated as the number of individuals of working age (15–64) per 100 older adults (65 and over). The municipality is the unit of analysis, and all data are drawn from ISTAT.[4]

Italy is among the Western countries that have experienced the sharpest increase in population aging over the past two decades. Accordingly, the national aggregate PSR has declined monotonically from 2002 to 2023, with the steepest reduction occurring in the last 12 years (Figure 1a). From an initial value of 358 in 2002, the PSR fell to 264 in 2023, meaning that the working-age population declined from about 3.5 times the size of the old-age population to only 2.5 times. This trend is consistent with previous studies on demographic aging in Italy (e.g., Tomassini and Lamura, 2009; De Rose et al., 2019).

– Insert Figure 1 about here –

A second key feature of the aging process is its uneven spatial distribution. At the macro-regional level, the gap in PSR values between the Center-North and the South has significantly narrowed, though it has not disappeared (Figure 1a). In 2002, the PSR in the South was 410, compared to 334 in the Center-North. This difference mainly reflected a lower share of older adults in the South (Figure 1b), since the working-age shares were initially similar in both areas (Figure 1c). The lower share of elderly in the South can be explained by higher fertility rates recorded there between the 1970s and early 1990s, which sustained the working-age population until about 2012 (Figure 1c). After that, the

[4] We use postcensal estimates for population size, births, and deaths for the period 2002–2018. From 2019 onward, we rely on ISTAT data from the Permanent Census. Migration flows for 2002–2023 are derived from changes of residence (ISTAT). To ensure demographic consistency, we also include a residual factor that accounts for administrative adjustments and, from 2019, Census over- and under-coverage. *Under-coverage* refers to the inclusion in the resident population of individuals who have provided "signals of life" in the area (from integrated administrative records such as tax filings, residence permits, etc.). *Over-coverage* refers to the exclusion of individuals who no longer show such signals of life from the resident population count.

working-age population in the South started to decline rapidly, while the old-age share increased more steeply (Figure 1b). As a result, the PSR gap between the two macro-areas narrowed substantially in the last decade: in 2023, the PSR was 279 in the South and 256 in the Center-North.

At a finer spatial scale, the reduction in heterogeneity is even clearer. The coefficient of variation of municipal PSR values decreased steadily over time, supporting the sigma-convergence hypothesis (Figure B1, Appendix B). Kernel density estimates also reveal substantial changes in the distribution of PSR across municipalities (Figure 2). While the left tail of the distribution (lowest PSR values) remained stable (Table B1, Appendix B), the right tail (highest PSR values) became thinner and shorter, showing increasing concentration around the interquartile range. This indicates that the national decline in PSR was largely driven by municipalities initially in the right tail—those with the highest PSR values—that gradually converged towards the national average. In 2002, 16.5% of municipalities (representing 23.6% of the total population) had PSR values above 450; by 2023, this share had fallen to just 0.5% of municipalities (0.5% of the population).

– Insert Figure 2 about here –

The spatiotemporal trend model[5] provides further insights. In 2002, low PSR values (in blue, Figure 3a) were concentrated in Liguria, Lower Piedmont, Tuscany, and mountainous areas of Abruzzo and Molise. By contrast, clusters of high PSR values (in yellow) were located in Lombardy, Veneto, the autonomous province of Bolzano, coastal areas of the South, and the Lazio region.[6] The low PSR levels in Liguria and Lower Piedmont are linked to deindustrialization following the decline of the Fordist model in

[5] The spatiotemporal trend model of the PSR is specified as follows: $PSR_{it} = \alpha + f(s_{1i}, s_{2i}, t) + \varepsilon_{it}$, where PSR_{it} is the potential support ratio of each Italian municipality i at time t; $f(s_{1i}, s_{2i}, t)$ is the spatiotemporal trend, representing a smooth interaction between latitude, longitude, and year; α is a constant term; and ε_{it} is the i.i.d. error term.
[6] Similar evidence is obtained using local Moran I and local G* statistics (see Appendix B).

the "Industrial Triangle" during the 1970s, combined with the rise of "Third Italy" industrial districts.[7] This shift triggered outmigration from Liguria and Piedmont towards other industrial districts, leading to population loss and aging in the former and higher PSR values in the latter (Bonifazi et al., 2021). At the same time, globalization fostered international migration, with foreign workers attracted to industrial areas. In Abruzzo and Molise, the early low PSR levels reflected persistent outmigration, especially after 1992 when state subsidies to local industries (via the "Cassa del Mezzogiorno") were abruptly withdrawn. Conversely, the higher PSR values observed in the coastal South reflect the concentration of working-age populations in these densely populated areas.

– Insert Figure 3 about here –

By 2023, the spatial distribution of PSR had shifted substantially. Figure 3b illustrates the widespread decline in PSR values across the country. The highest PSR values are now confined to the autonomous province of Bolzano—long recognized for its high fertility and low aging rates—and to some metropolitan areas in the Center and South, including Rome, Naples, Catania, and parts of coastal Puglia.

4. Econometric Results

In this section, we present the results of the absolute and conditional beta convergence analyses (Eqs. 13–14). In the case of absolute convergence, a negative beta coefficient indicates that municipalities with initially high PSR values tend to catch up with those with initially low values. In the conditional specification, a negative coefficient suggests that PSR values converge across municipalities with similar observable and unobservable characteristics.

[7] The expression "industrial triangle" refers to the three major cities (Milan, Turin, and the seaport of Genoa), where the heavy manufacturing sectors were concentrated until the first oil shock in the early 1970s which led to the crisis of the Fordist model. The expression "Third Italy" describes specialized clusters of small-and-medium-sized firms (so-called industrial districts) in the northeast and in the Center that emerged during the 1970s.

Figures 4–6 display the time-varying coefficients,[8] while Table 1 reports the mean values of the decomposition. Figures 5 and 6 provide a further breakdown of the PSR changes, distinguishing between the first-step (old-age vs. working-age) and second-step (cohort turnover, mortality, and migration) components. The horizontal axis shows the years, and the vertical axis the estimated beta coefficients (panel a: absolute convergence; panel b: conditional convergence). Dashed lines represent 95% confidence intervals. Figure 7 adds the decomposition of net migration into its internal and international components.

– Insert Table 1 here –

4.1 Beta Convergence Analysis: Baseline Results

When the overall change in PSR is used as the dependent variable (black line, Figure 4a), all estimated beta coefficients are negative, with a mean value of –0.044 (one-percentage-point increase in the PSR at time $t-1$ leads to an average decrease of 4.4 percent in the PSR at time t). This indicates absolute convergence: municipalities with higher initial PSR values experienced faster declines, thus catching up with those with lower initial values. The effect is robust to the inclusion of spatiotemporal heterogeneity (Figure 4b).

– Insert Figure 4 about here –

The dynamics were not constant over time. In the early 2000s, beta values were closer to zero, reflecting slower convergence, with a peak in 2009. Convergence accelerated thereafter, consistent with the rapid PSR decline observed in Southern municipalities (Figure C1, Appendix C). This acceleration suggests that regional disparities in demographic aging narrowed substantially in the last decade.

[8] Given the large difference in the size of municipalities, in all regressions spatial units have been weighted using the total population as weight.

4.2 First-step Decomposition

Figure 4 also decomposes the convergence process into the contributions of the old-age and working-age populations. The results clearly show that convergence is mainly driven by the old-age component. The corresponding beta coefficients are consistently negative, with mean values (β^o in Table 1) of –0.054 (absolute) and –0.056 (conditional). By contrast, the working-age component displays positive beta coefficients, with means (β^w in Table 1) of 0.010 and 0.016, implying a diverging effect that partially offsets the overall convergence.

The spatial patterns reinforce this interpretation. Figure C2 (Appendix C) shows that in both 2002–2012 and 2012–2023, changes in the old-age component closely track the overall PSR decline, while the working-age component contributed to divergence only in the early period. Between 2002 and 2012, municipalities with initially high PSR values—such as Lombardy, Veneto, Bolzano, and some southern coastal zones—recorded stronger working-age dynamics (Figure C2, panel c), which slowed convergence. In contrast, during 2012–2023, working-age changes turned negative almost everywhere, particularly in the South, accelerating convergence (Figure C2, panel d).

4.3 Second-step Decomposition

We now decompose the working-age component into cohort turnover, mortality, and migration (Figure 5). The mortality component consistently shows a convergent effect, but its magnitude is negligible (average beta around –0.002). The cohort turnover component, by contrast, exerts a diverging effect, with average betas of 0.014 (absolute) and 0.008 (conditional).[9]

[9] The statistical adjustment component plays also a marginal role all over the period.

The migration component is more complex. Absolute convergence estimates suggest a small convergent effect (average β^{mg} –0.001), but this disappears once unobserved heterogeneity is controlled for. In the conditional specification, the migration beta is positive (0.010), confirming that migration has a diverging effect, as expected. Hence, we focus on the conditional results.

– Insert Figure 5 about here –

The diverging impact of cohort turnover was strongest in the early 2000s, consistent with the younger age structure in the South. However, as the fertility advantage of the South waned, this effect weakened and by 2012–2023 was only visible in Bolzano and a few southern municipalities (Figure C3, panel b). Migration, on the other hand, generated strong divergence in 2002–2012: municipalities with higher initial PSR values, such as Lombardy, Veneto, and Lazio's coastal areas, benefited from net inflows (Figure C3, panel c), while many southern municipalities experienced net outflows, which exacerbated aging. After 2012, the effect attenuated: inflows into prosperous municipalities became less pronounced, while outflows from the South persisted (Figure C3, panel d).

4.4 Migration Decomposition

Finally, Figure 6b decomposes the migration effect into internal and international flows, by Italians and foreigners. The divergent impact of migration in the first decade, and its subsequent attenuation, is almost entirely explained by the internal migration of Italians (blue line; see also Figure C6, panels a–b). International migration of foreigners (brown line) was more erratic but also contributed to divergence (Figure C6, panels c–d). Other components—internal migration of foreigners and international migration of Italians—had negligible effects.

– Insert Figure 6 about here –

Overall, these results confirm that while old-age dynamics are the main driver of convergence in aging across Italian municipalities, migration continues to shape spatial heterogeneity. Internal migration of Italians, in particular, has reinforced territorial imbalances, contributing to demographic fragility in peripheral areas and rejuvenation in urban centers.

5. Conclusions and Policy Implications

Italy faces a profound demographic challenge, with one of the fastest-aging populations worldwide, ranking just behind Japan and Korea. Declining fertility, rising life expectancy, and regional disparities have reduced spatial heterogeneity in municipal age structures, producing convergence toward an undesirable equilibrium in the Potential Support Ratio (PSR). This places increasing pressure on the working-age population to sustain the elderly.

Using a variable-coefficient beta convergence approach on municipality-level data (2002–2023), we find an accelerated convergence in the past decade, mainly driven by the elderly (65+) in the South, while the initially divergent effect of the working-age group (15–64) has faded. Net migration, once a diverging force, has recently supported convergence.

Migration is therefore crucial to mitigating aging in Italy, where fertility and mortality changes require decades to alter age structures. Yet migration alone cannot provide a durable solution and must be paired with policies that increase fertility and improve the quality of life for older adults. More effective immigration policies could help sustain the PSR, though political resistance limits their scope. The *Decreto Flussi* has admitted about

800,000 workers in the past two decades, mainly in construction, agriculture, and care services, but such measures address only immediate shortages. Long-term strategies require integration policies that enhance language skills, economic participation, cultural assimilation, and family reunification.

Immigrants also contribute through higher fertility: in 2023, foreign women averaged 1.79 children versus 1.14 among Italians. This underlines the need for comprehensive family policies. Recent innovations, such as the *Assegno Unico Universale* and expanded childcare, represent progress but remain uneven across regions. Evidence shows that single measures have only modest, short-lived effects (Gauthier, 2007; Guetto et al., 2023), while coherent mixes of financial incentives, childcare, and parental leave yield more lasting impacts.

Beyond fertility, strategies must target working-age cohorts and promote active aging to transform older populations into social and economic resources. Disease prevention, incentives for firms to retain older workers, and digital literacy programs can reduce welfare costs and enhance participation.

While national-level interventions are crucial, our spatial analysis underscores the importance of place-based policies tailored to local contexts. Some regions, such as Liguria and Low Piedmont, entered the sample period with low PSR values due to deindustrialization in the 1970s. Others, despite starting from stronger positions, have since converged to the undesirable equilibrium because of weak cohort turnover or persistent outmigration. By contrast, areas benefiting from internal and international immigration of working-age individuals have sustained relatively higher PSR levels. Addressing such heterogeneity requires aligning demographic policies with the specific needs and economic profiles of different territories.

This is particularly urgent in peripheral areas experiencing the continuous outmigration of young, often highly educated individuals. Investment in infrastructure, community development, and support for small and medium-sized enterprises can foster growth and counter population decline. In this vein, the National Strategy for Inner Areas seeks to improve access to essential services—healthcare, education, and mobility—while promoting economic and social development through integrated, place-based initiatives. Covering 72 pilot areas, the strategy aims to enhance innovation, strengthen local skills, and improve quality of life in rural and remote communities. Within this framework, policies to retain skilled workers and encourage the return of expatriates are critical, including tax incentives, career opportunities, and reintegration support (Coppola & Di Iorio, 2013).

Finally, intergenerational imbalances, socio-economic inequalities, and demographic decline are also reshaping metropolitan realities, producing peri-urbanization and segregation dynamics. The former reflects the outward expansion of households and firms into suburban or rural zones in response to housing affordability, while the latter manifests in uneven spatial distributions of population by socio-economic and cultural characteristics. Italian metropolitan areas are responding with policies of urban regeneration—redeveloping suburbs to foster integration and attract investment—and measures for social inclusion. Such interventions are essential to reduce center–periphery disparities and promote cohesive, sustainable urban development.

References

Backman, M., & Karlsson, C. (2024). Ageing places: convergence and the role of the foreign population, *Regional Studies*, 58:5, 922-937.

Barro, R. J., Sala-i-Martin, X., Blanchard, O. J., & Hall, R. E. (1991). Convergence across states and regions. *Brookings papers on economic activity*, 107-182.

Basile R., Basso S., Miccoli S., Reynaud C. (2022), Ageing population in Italy: a space-time analysis, *Rivista Italiana di Economia, Demografia e Statistica*, 76(2), 77-88

Bloom, D. E., S. Chatterji, P. Kowal, Sherlock P.L., McKee M., Rechel B., Rosemberg L., Smith J.P. (2015): "Macroeconomic implications of population ageing and selected policy responses," The Lancet, 385(9968), 649–657.

Bloom, D., Canning, D., & Sevilla, J. (2003). *The demographic dividend: A new perspective on the economic consequences of population change*. Rand Corporation.

Bloom, D. E., and Luca, D. L. (2016). The global demography of aging: facts, explanations, future. In *Handbook of the Economics of Population Aging* (Vol. 1, pp. 3-56). North-Holland.

Boeri, T., Gamalerio, M., Morelli, M., and Negri, M. (2024). Pay-as-they-get-in: attitudes toward migrants and pension systems. *Journal of Economic Geography*, 24(1), 63-78.

Bonifazi, C., Heins, F., Licari, F., & Tucci, E. (2021). The regional dynamics of internal migration intensities in Italy. *Population, Space and Place*, *27*(7).

Chen, C., Li, J., Huang, J. (2022), Spatial–Temporal Patterns of Population Aging in Rural China. *International Journal of Environmental Research and Public Health*, 19, 1-18

Coale, A.J. (1989). Demographic Transition. In: Eatwell, J., Milgate, M., Newman, P. (eds) Social Economics. The New Palgrave. Palgrave Macmillan, London. https://doi.org/10.1007/978-1-349-19806-1_4

Coleman, D. A. (1995). International migration: demographic and socioeconomic consequences in the United Kingdom and Europe. *International Migration Review*, *29*(1), 155-206.

Coppola, L., & Di Iorio, F. (2013). The impact of the economic crisis on fertility in Italy. *European Journal of Population*, 29(1), 37-60.

Craveiro, D., De Oliveira, I. T., Gomes, M. S., Malheiros, J., Moreira, M. J. G., & Peixoto, J. (2019). Back to replacement migration. *Demographic Research*, *40*, 1323-1344.

Dalla-Zuanna, G., e McDonald, P. F. (2023). A change of direction for family policy in Italy: some reflections on the general family allowance (GFA), *Genus*, 79(1), 12.

De Rose, A., F. Racioppi, P. Checcucci, M. F. Arezzo, and C. Polli (2019): The workforce aging and challenges for policy and for business. The case of Italy, *Review of European Studies*, 11, 60.

Ediev, D. M. (2014): Why increasing longevity may favour a PAYG pension system over a funded system, *Population Studies*, 68(1), 95–110. F.

Eilers, P. H., & Marx, B. D. (1996). Flexible smoothing with B-splines and penalties. *Statistical Science*, *11*(2), 89-121.

Eurostat (2023), "EU median age increased by 2.3 years since 2013, 15 February 2024. https://ec.europa.eu/eurostat/web/products-eurostat-news/w/ddn-20240215-

1#:~:text=EU's%20old%2Dage%20dependency%20ratio,when%20it%20was%20at%2027.7%25.

Feldstein, M. S. (2006): The effects of the ageing European population on economic growth and budgets: implications for immigration and other policies, *NBER Working Paper* No. 12736

Findlay, A. M., and Wahba, J. (2013). Migration and demographic change. *Population, Space and Place*, *19*(6), 651-656.

Gauthier, A. H. (2007). The impact of family policies on fertility in industrialized countries: a review of the literature. *Population research and policy review*, *26*, 323-346.

Ghio, D., Goujon, A., and Natale, F. (2022). Assessing the demographic impact of migration on the working-age population across European territories. *Demographic Research*, *46*, 261-272.

Gruber, J., and D. Wise (1999): "Social security programs and retirement around the world," *Research in labor economics*, 18(1), 40.

Gutiérrez Posada, D., Rubiera Morollón, F., & Viñuela, A. (2018). Ageing places in an ageing country: The local dynamics of the elderly population in Spain. *Tijdschrift voor Economische en Sociale Geografie*, 109(3), 332–349.

Guetto, R., Alderotti, G., e Vignoli, D. (2023). Can Policy Reforms Enhance Fertility? An Ex-Ante Evaluation through Factorial Survey Experiments, *Università degli Studi di Firenze, Working Paper Series 2003/08, Dipartimento di Statistica, Informatica, Applicazioni" G. Parenti".*

Istat (2024), Demographic indicators – Years 2023. *https://www.istat.it/en/archivio/295592*

Kashnitsky, I., J. De Beer, and L. Van Wissen (2017): “Decomposition of regional convergence in population aging across Europe,” Genus, 73, 1–25.

Lee, D. J., & Durbán, M. (2011). P-spline ANOVA-type interaction models for spatio-temporal smoothing. *Statistical modelling*, *11*(1), 49-69.

Leers, T., Meijdam, L., & Verbon, H. A. (2004). Ageing, migration and endogenous public pensions. *Journal of Public Economics*, *88*(1-2), 131-159.

Mahon, J., and C. C. Millar (2014): ManAGEment: the challenges of global age diversity for corporations and governments, *Journal of Organizational Change Management*, 27(4), 553–568.

Monturano, G., Resce, G., & Ventura, M. (2023). The Impact of Italy's Strategy for Inner Areas on Depopulation and Industrial Growth: A Staggered Diff-in-Diff Analysis with Spatial Spillover Effects. *Available at SSRN 4575900*.

Nagarajan, N. R., Teixeira, A. A., and Silva, S. T. (2021). Ageing population: identifying the determinants of ageing in the least developed countries. *Population Research and Policy Review*, *40*, 187-210.

Neumann, U. (2013). Are my neighbours ageing yet? Local dimensions of demographic change in German cities. *Journal of Population Ageing*, *6*, 189-209.

Peri, G. (2020). Immigrant Swan Song. *Finance & Development*.

Prenzel, P. (2021). Are old regions less attractive? Interregional labour migration in a context of population ageing. *Papers in Regional Science*, *100*(6), 1429-1448.

Pritchett, L. (2023). The Demographic Future of Europe: Immigration and Aging. European Journal of Demography, 58(3), 512-534.

Smailes, P., Griffin, T., & Argent, N. (2014). Demographic Change, Differential Ageing, and Public Policy in Rural and Regional Australia: A Three-State Case Study. *Geographical Research*, *52*(3), 229-249.

Tomassini, C., & Lamura, G. (2009). Population ageing in Italy and southern Europe. In *International handbook of population aging* (pp. 69-89). Dordrecht: Springer Netherlands.

United Nations (UN) (2000). *Replacement migration: Is it a solution to declining and ageing populations?* New York: United Nations

Vlandas, T., McArthur, D., & Ganslmeier, M. (2021). Ageing and the economy: a literature review of political and policy mechanisms. *Political Research Exchange*, *3*(1), 1932532.

World Health Organization (2020): "Ageing," WHO.

Wu, L., Huang, Z., and Pan, Z. (2021). The spatiality and driving forces of population ageing in China. *Plos one*, *16*(1), e0243559.

Wu, Y., Song, Y., & Yu, T. (2019). Spatial differences in China's population aging and influencing factors: The perspectives of spatial dependence and spatial heterogeneity. *Sustainability*, *11*(21), 5959.

Yang, L., Zhao, K., & Fan, Z. (2019). Exploring determinants of population ageing in Northeast China: From a socio-economic perspective. *International Journal of Environmental Research and Public Health*, *16*(21), 4265.

Zaiceva, A. (2014). The impact of aging on the scale of migration. *IZA World of labor*.

Zhang, X., & Han, H. (2023). Spatiotemporal Dynamic Characteristics and Causes of China's Population Aging from 2000 to 2020. *Sustainability*, *15*(9), 7212.

FIGURE 1 Demographic trends: Center-North and South aggregated statistics

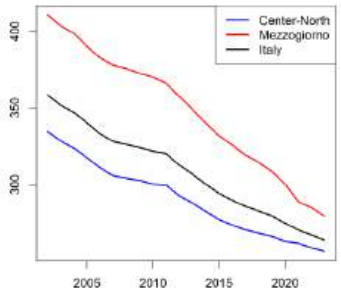

(a) PSR*100

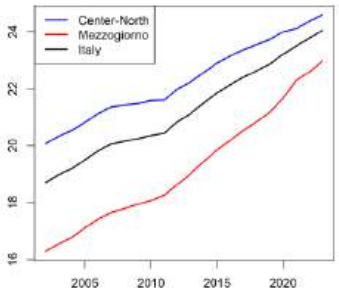

(b) O/P*100

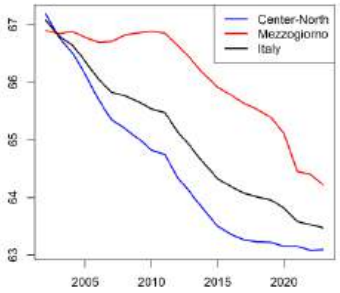

(c) W/P*100

Source: our elaboration on Istat data.

FIGURE 2 Municipality PSR: univariate density estimates

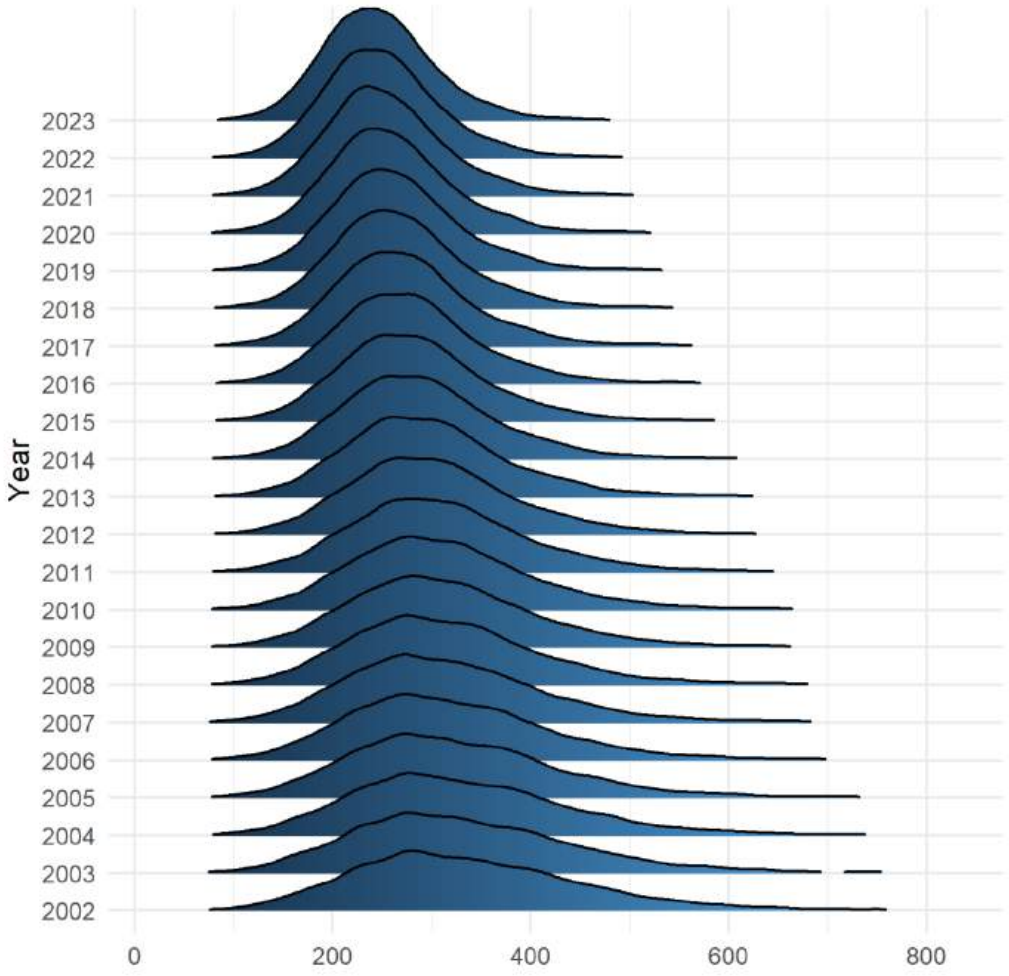

Source: our elaboration on Istat data.

FIGURE 3 Spatiotemporal trend analysis

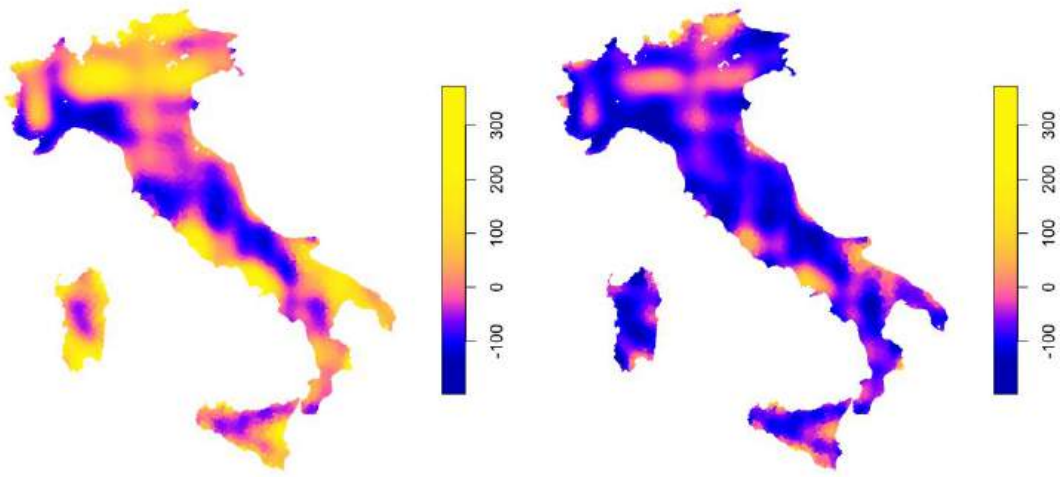

(a) 2002 (b) 2023

Source: our elaboration on Istat data.

Table 1 Beta-convergence analysis: mean values of time varying beta parameters

Beta coefficient	Absolute	Conditional
Overall beta		
β	-0,044	-0,041
First step decomposition		
β^{o}	-0,054	-0,056
β^{w}	0,010	0,016
Second step decomposition		
β^{ct}	0,014	0,008
β^{mg}	-0,001	0,010
β^{dt}	-0,002	-0,001
β^{Δ}	-0,001	-0,002

Source: our elaboration on Istat data.

FIGURE 4 Beta-convergence: First step

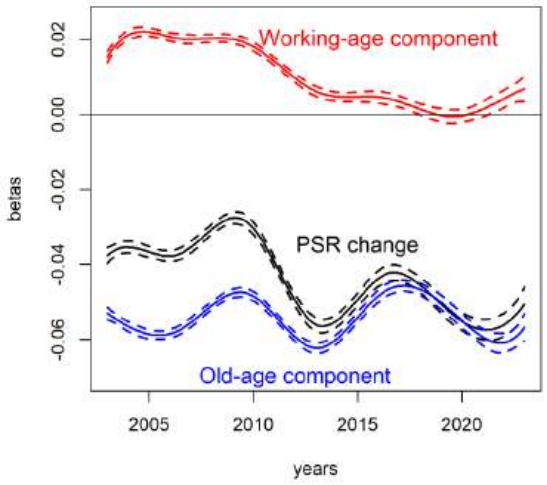

(a) Absolute convergence

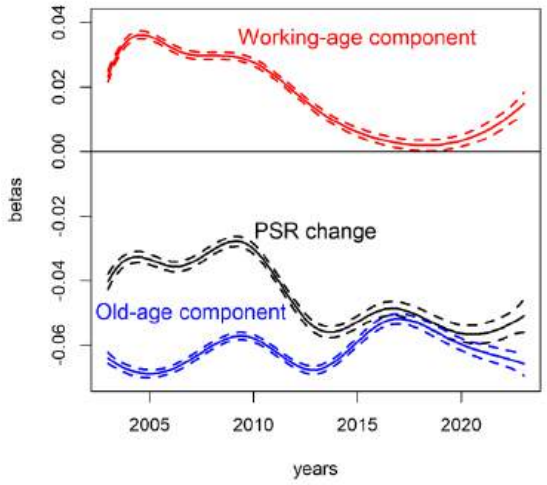

(b) Conditional convergence

Source: our elaboration on Istat data.

FIGURE 5 Beta-convergence: Second step

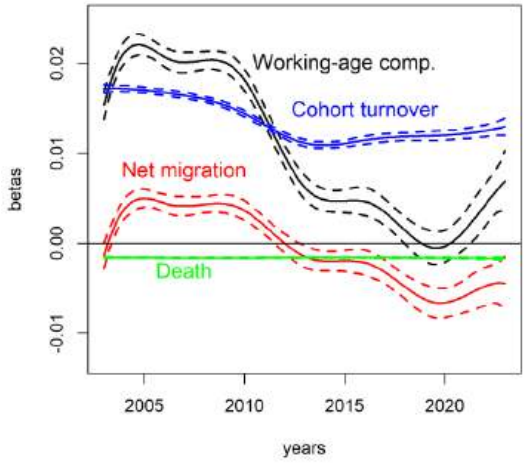

(a) Absolute convergence

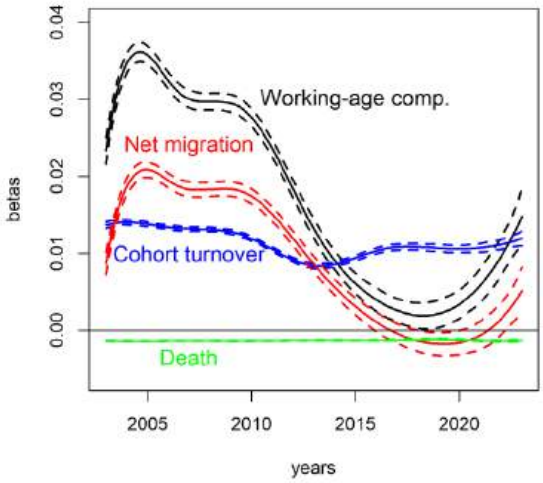

(b) Conditional convergence

Source: our elaboration on Istat data.

FIGURE 6 Decomposing the net-migration effect

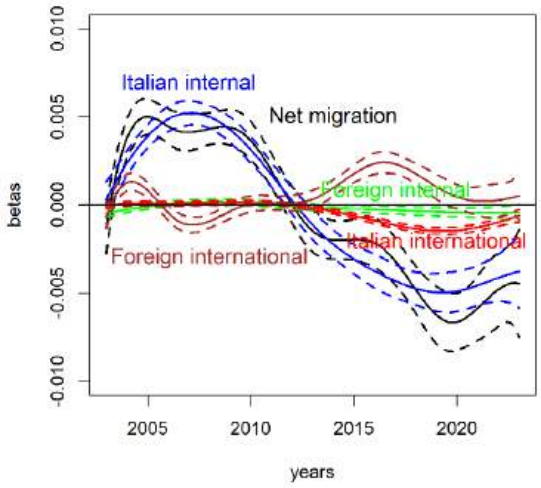

(a) Absolute convergence

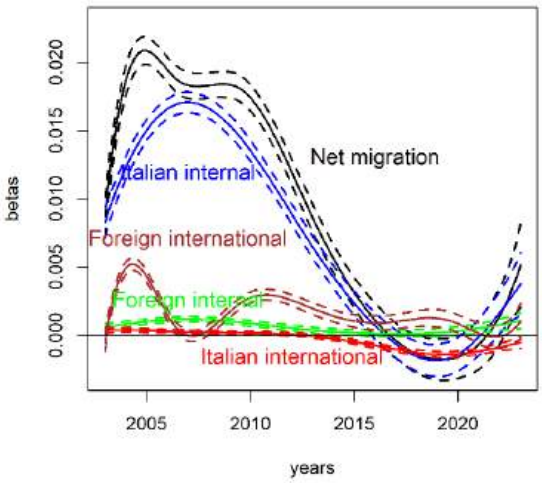

(b) Conditional convergence

Source: our elaboration on Istat data.

1 Appendix A: Penalized splines methodology

1.1 Penalized splines as mixed models

The method of penalized regression relies on representing unknown functions using a basis, coupled with a penalty on the likelihood to regulate the smoothness of the curve or surface. Specifically, we adopt the technique introduced by Eilers and Marx (1996), utilizing cubic B-splines (De Boor, 1977) as basis functions, and imposing penalties based on the second-order differences of adjacent coefficients. Our starting point is a straightforward scenario where the mean of the response variable is an unspecified function of the single covariate t:

$$y_{it} = f(t) + \varepsilon_{it} \quad \varepsilon \sim N(0, \sigma^2), \tag{1}$$

Afterwards, the representation of the smooth function is given by:

$$f(\mathbf{t}) = \sum_{j=1}^{c} B_j(\mathbf{t})\theta_j \quad j = 1, ..., c, \tag{2}$$

with B_j represents a B-spline basis function, and θ_j is a component within a vector of regression coefficients with a length of c (the number of knots utilized for constructing the basis). The curve's smoothness is regulated by a quadratic penalty term. This term is usually comparable to the integral of squared second derivatives of the function, but its calculation can be challenging, especially in the context of interactions.

Therefore, in line with Eilers and Marx (1996), we opt for second-order differences among neighboring coefficients, leading to the subsequent penalized regression problem:

$$\|\mathbf{y} - \mathbf{B}\boldsymbol{\theta}\|^2 + \lambda \sum_j (\Delta^2 \theta_j)^2. \tag{3}$$

In this context, $\mathbf{B}$ is a matrix that encompasses B-spline basis functions represented by B_j in columns and Δ^2 refers to the second-order difference operator. When expressed in matrix form, the penalty term transforms into $\boldsymbol{\theta}'\mathbf{P}\boldsymbol{\theta}$, where $\mathbf{P} = \lambda \mathbf{D}'\mathbf{D}$. Here, $\mathbf{D}$ signifies the matrix of second-order differences, and λ serves as the smoothing parameter, dictating the degree of smoothness.

It is readily apparent that the estimated smooth function is expressed as:

$$\widehat{f}(\mathbf{t}) = \mathbf{B}(\mathbf{B}'\mathbf{B} + \lambda \mathbf{D}'\mathbf{D})^{-1}\mathbf{B}\mathbf{y}. \tag{4}$$

The estimation of the unknown function is contingent on the smoothing parameter λ, emphasizing the necessity for optimal parameter selection. An approach to determine the ideal smoothing parameter involves reparameterizing the penalized spline model into a mixed model, as proposed by Eilers, Currie, and Durbán (2006). This transformation includes converting B-spline bases into a new model basis, denoted as $\mathbf{B} \rightarrow [\mathbf{X} : \mathbf{Z}]$, and the coefficients $\boldsymbol{\theta} \rightarrow (\boldsymbol{\beta}, \boldsymbol{\alpha})'$. This concept is rooted in recognizing that the minimization problem in equation 4 mirrors the minimization criterion in a random effects model structured as:

$$\mathbf{y} = \mathbf{B}\boldsymbol{\theta} + \boldsymbol{\varepsilon}. \tag{5}$$

In this scenario, $\mathbf{B}$ represents a matrix comprising B-spline bases, and $\boldsymbol{\theta}$ is a vector of regression parameters slated for estimation through a penalized sum of squares:

$$(\mathbf{y}-\mathbf{B}\boldsymbol{\theta})'(\mathbf{y}-\mathbf{B}\boldsymbol{\theta})+\boldsymbol{\theta}'\mathbf{P}\boldsymbol{\theta}. \tag{6}$$

Nevertheless, the penalty matrix P exhibits singularity (with 2 zero eigenvalues), resulting in a degenerate distribution. One viable resolution involves rephrasing the model as:

$$\mathbf{B}\theta = \mathbf{X}\beta + \mathbf{Z}\alpha. \tag{7}$$

This restructuring breaks down the fitted values into a sum of an unpenalized polynomial component $\mathbf{X}\boldsymbol{\beta}$ and a penalized nonlinear smooth term $\mathbf{Z}\boldsymbol{\alpha}$. Executing this transformation requires determining an orthogonal transformation matrix $\mathbf{T}$, ensuring $\mathbf{BT} = [\mathbf{X} : \mathbf{Z}]$ and $\mathbf{T}'\boldsymbol{\theta} = (\boldsymbol{\beta}, \boldsymbol{\alpha})'$.

Numerous options exist for this matrix selection; we opt for one based on the singular value decomposition of the penalty matrix $\mathbf{P} = \lambda\mathbf{D}'\mathbf{D}$, which is:

$$\mathbf{D}'\mathbf{D} = \mathbf{U}\boldsymbol{\Sigma}\mathbf{U}', \tag{8}$$

where $\boldsymbol{\Sigma}$ forms a diagonal matrix encompassing the eigenvalues of $\mathbf{D}'\mathbf{D}$, featuring 2 zero eigenvalues. The matrix $\mathbf{U}$, containing the corresponding eigenvectors, can be decomposed into two segments: $\mathbf{U}_n$ of dimension $c \times 2$ containing the null-part eigenvectors and $\mathbf{U}_s$ of dimension $c \times (c-2)$ (where c denote the rank of the basis and 2 is the order of the penalty), containing the non-null-part eigenvectors. It is worth noting that $\boldsymbol{\Sigma}$ can be express as $\boldsymbol{\Sigma} = blockdiag\left(\mathbf{0}_2, \tilde{\boldsymbol{\Sigma}}\right)$. Here, $\tilde{\boldsymbol{\Sigma}}$ is a diagonal matrix that contains the non-zero eigenvalues of $\mathbf{D}'\mathbf{D}$ and $\mathbf{0}_2$ is a 2×2 matrix of zeroes. Therefore, the transformation matrix $\mathbf{T}$ can be defined as:

$$\mathbf{T} = [\mathbf{U}_n : \mathbf{U}_s\tilde{\boldsymbol{\Sigma}}^{-1/2}]. \tag{9}$$

In this context, the matrices for fixed and random effects are denoted as $\mathbf{X} = \mathbf{B}\mathbf{U}_n$ and $\mathbf{Z} = \mathbf{B}\mathbf{U}_s$, respectively. Additionally, with this transformation matrix, the updated coefficients are expressed as $\boldsymbol{\beta} = \mathbf{U}_n'\boldsymbol{\theta}$ and $\boldsymbol{\alpha} = \mathbf{U}_s'\tilde{\boldsymbol{\Sigma}}^{-1/2}\boldsymbol{\theta}$. The fixed effect matrix $\mathbf{X}$ can be substituted with any sub-matrix, ensuring $[\mathbf{X} : \mathbf{Z}]$ maintains full rank, and $\mathbf{X}'\mathbf{Z} = \mathbf{0}$ (indicating orthogonality between $\mathbf{X}$ and $\mathbf{Z}$). Moreover, the penalty term $\boldsymbol{\theta}'\mathbf{P}\boldsymbol{\theta}$ is transformed into $\boldsymbol{\alpha}'\mathbf{F}\boldsymbol{\alpha}$, where $\mathbf{F} = \lambda\mathbf{I}$. This is attributed to the orthogonality of $\mathbf{T}$ and $(\boldsymbol{\beta}, \boldsymbol{\alpha})' = \mathbf{T}'\boldsymbol{\theta}$. Consequently, given the revised basis and penalty, the penalized sum of squares $(\mathbf{y}-\mathbf{B}\boldsymbol{\theta})'(\mathbf{y}-\mathbf{B}\boldsymbol{\theta})+\boldsymbol{\theta}'\mathbf{P}\boldsymbol{\theta}$ becomes:

$$(\mathbf{y}-\mathbf{X}\boldsymbol{\beta}-\mathbf{Z}\boldsymbol{\alpha})'(\mathbf{y}-\mathbf{X}\boldsymbol{\beta}-\mathbf{Z}\boldsymbol{\alpha})+\lambda\boldsymbol{\alpha}'I_{c-2}\boldsymbol{\alpha}. \tag{10}$$

This corresponds to the joint log-likelihood of a linear mixed model:

$$\mathbf{y} = \mathbf{X}\boldsymbol{\beta}+\mathbf{Z}\boldsymbol{\alpha}+\boldsymbol{\epsilon}, \quad \boldsymbol{\alpha} \sim \mathcal{N}(\mathbf{0}, \mathbf{G}), \tag{11}$$

where $\mathbf{G}$ is defined as $\sigma_v^2\mathbf{I}_{c-2}$ and λ is expressed as σ^2/σ_v^2. Consequently, the estimation of the smoothing parameters involves estimating the variance components within the mixed model.

1.2 Penalized splines models with interactions

We also allow the smooth time trend $f(t)$ to interact with the continuous term x_{it}. So, the final model will be:

$$y_{it} = \alpha + f(t) + f(t)x_{it} + \varepsilon_{it}. \tag{12}$$

The concept revolves around the notion that the linear regression coefficient for x_{it} undergoes smooth variations with t. No additional theory is necessary to identify the interaction term (Wood, 2010). Simply put, we need to multiply each element of the rows of the model matrix for $f(t)$ by x_{it} for each i, leaving everything else unaltered.

1.3 Spatiotemporal ANOVA model

In numerous scenarios, the spatio-temporal trend to be estimated can be complex (Mínguez, Basile, and Durbán, 2020), and relying solely on a single multidimensional smooth function might not offer sufficient flexibility to adequately capture the data's structure. To address this challenge, Lee and Durbán (2011) proposed an ANOVA-type decomposition of $g(s_1, s_2, t)$. This decomposition allows for the identification of spatial and temporal main effects, as well as second- and third-order interactions between them:

$$g(s_1, s_2, t) = g_1(s_1) + g_2(s_2) + g_t(t) + g_{1,2}(s_1, s_2) + g_{1,t}(s_1, t) + g_{2,t}(s_2, t) + g_{1,2,t}(s_1, s_2, t) \quad (13)$$

Thus, our attention is directed towards the subsequent model:

$$\begin{aligned} \mathbf{y} \quad = \quad & g_1(\mathbf{s_1}) + g_2(\mathbf{s_2}) + g_t(\mathbf{t}) + \\ & g_{1,2}(\mathbf{s_1}, \mathbf{s_2}) + g_{1,t}(\mathbf{s_1}, \mathbf{t}) + \\ & g_{2,t}(\mathbf{s_2}, \mathbf{t}) + \\ & g_{1,2,t}(\mathbf{s_1}, \mathbf{s_2}, \mathbf{t}) + \varepsilon \end{aligned} \quad (14)$$

The geoadditive terms $g_1(\mathbf{s_1})$, $g_2(\mathbf{s_2})$ and $g_{1,2}(\mathbf{s_1}, \mathbf{s_2})$, representing the two 1d smooth functions of latitude and longitude and the 2d smooth function, work as control functions to filter the spatial trend out of the residuals, and transfer it to the mean response in the model specification (Basile, Durbán, Mínguez, Montero, and Mur, 2014). The smooth time trend, $g_t(\mathbf{t})$, and the smooth interactions between space and time, $g_{1,t}(\mathbf{s_1}, \mathbf{t})$, $g_{2,t}(\mathbf{s_2}, \mathbf{t})$, and $f_{1,2,t}(\mathbf{s_1}, \mathbf{s_2}, \mathbf{t})$, work as control functions to capture the heterogeneous effect of common shocks.

Expressing the model in matrix notation, we have:

$$\mathbf{y} = \mathbf{B}\boldsymbol{\theta} + \boldsymbol{\epsilon} \qquad \boldsymbol{\epsilon} \sim N\left(\mathbf{0}, \frac{\sigma^2}{1-\phi^2}\boldsymbol{\Omega}\right) \quad (15)$$

The regression matrix for the aforementioned model will consist of the concatenation of B-spline bases for every smooth term within the model:

$$\mathbf{B} = [\mathbf{1}|\mathbf{B}_{s_1}|\mathbf{B}_{s_2}|\mathbf{B}_{s_1}\square\mathbf{B}_{s_2}|\mathbf{B}_{s_1} \otimes \mathbf{B}_t|\mathbf{B}_{s_2} \otimes \mathbf{B}_t|(\mathbf{B}_{s_1}\square\mathbf{B}_{s_2}) \otimes \mathbf{B}_t]. \quad (16)$$

Here, $\mathbf{B}_{s_1}$, $\mathbf{B}_{s_2}$ and $\mathbf{B}_t$ represent the marginal B-spline bases for the spatial coordinates $(\mathbf{s_1}, \mathbf{s_2})$ and time $(\boldsymbol{t})$, while symbol $\square$ signifies the row-wise tensor product defined as:

$$\mathbf{B}_i\square\mathbf{B}_j = (\mathbf{B}_i \otimes \mathbf{1}'_{c_i}) * (\mathbf{1}'_{c_j} \otimes \mathbf{B}_j), \quad (17)$$

where $\mathbf{1}$ denotes a column vector of ones, c_i represents the rank of $\mathbf{B}_i$, and $\otimes$ and $*$ denote the Kronecker and element-wise matrix products, respectively.

The penalty matrix is structured as block-diagonal, with each block corresponding to different terms in the model:

- $\lambda_i\mathbf{D}'_i\mathbf{D}_i$ for main effects;
- $\lambda_i\mathbf{D}'_i\mathbf{D}_i \otimes \mathbf{I}_{c_k} + \lambda_k\mathbf{I}_{c_i} \otimes \mathbf{D}'_k\mathbf{D}_k$ for the second-order interactions;

- $\lambda_i \mathbf{D}_i'\mathbf{D}_i \otimes \mathbf{I}_{c_k} \otimes \mathbf{I}_{c_l} + \lambda_k \mathbf{I}_{c_i} \otimes \mathbf{D}_k'\mathbf{D}_k \otimes \mathbf{I}_{c_j} + \lambda_l \otimes \mathbf{I}_{c_i} \otimes \mathbf{I}_{c_k} \otimes \mathbf{D}_l'\mathbf{D}_l$ for the three-way interaction.

In such instances, various constraints must be enforced, as the subspace spanned by any product $\mathbf{B}_i \otimes \mathbf{B}_j$ encompasses the space spanned by the marginal bases $\mathbf{B}_i$ and $\mathbf{B}_j$. The mixed model reparameterization inherently incorporates these required constraints. To determine this reparameterization, following Lee (2010), a new transformation matrix is needed. Subsequently, the model is expressed as:

$$\mathbf{y} = \mathbf{X}\beta + \mathbf{Z}\alpha + \varepsilon \qquad \alpha \sim \mathbf{N}(\mathbf{0}, \mathbf{G}), \tag{18}$$

where $\mathbf{X}_k$ and $\mathbf{Z}_k$ (with k taking values s_1, s_2, t) represent the mixed model matrices acquired through the reparameterization of the marginal basis detailed in Appendix A. The two matrices are defined as:

$$\begin{aligned} \mathbf{X} &= [(\mathbf{X}_{s_1} \square \mathbf{X}_{s_2}) \otimes \mathbf{X}_t] \\ \mathbf{Z} &= [(\mathbf{Z}_{s_1} \square \mathbf{X}_{s_2}) \otimes \mathbf{X}_t | (\mathbf{X}_{s_1} \square \mathbf{Z}_{s_2}) \otimes \mathbf{X}_t | (\mathbf{X}_{s_1} \square \mathbf{X}_{s_2}) \otimes \mathbf{Z}_t | (\mathbf{Z}_{s_1} \square \mathbf{Z}_{s_2}) \otimes \mathbf{X}_t | \\ &\quad (\mathbf{Z}_{s_1} \square \mathbf{X}_{s_2}) \otimes \mathbf{Z}_t | (\mathbf{X}_{s_1} \square \mathbf{Z}_{s_2}) \otimes \mathbf{Z}_t | (\mathbf{Z}_{s_1} \square \mathbf{Z}_{s_2}) \otimes \mathbf{Z}_t] \end{aligned} \tag{19}$$

The covariance matrix of random effects, denoted as $\mathbf{G}$, is structured such that:

$$\begin{aligned} \mathbf{G}^{-1} = \text{blockdiag} \Bigg(& \mathbf{0}, \frac{1}{\sigma^2_{v_1}}\mathbf{\Lambda}_1, \frac{1}{\sigma^2_{v_2}}\mathbf{\Lambda}_2, \frac{1}{\sigma^2_{v_3}}\mathbf{\Lambda}_3, \frac{1}{\sigma^2_{v_4}}\mathbf{\Lambda}_4 + \frac{1}{\sigma^2_{v_5}}\mathbf{\Lambda}_5, \frac{1}{\sigma^2_{v_6}}\mathbf{\Lambda}_6 + \frac{1}{\sigma^2_{v_7}}\mathbf{\Lambda}_7, \frac{1}{\sigma^2_{v_8}}\mathbf{\Lambda}_8 = \frac{1}{\sigma^2_{v_9}}\mathbf{\Lambda}_9, \\ & \frac{1}{\sigma^2_{v_{10}}}\mathbf{\Lambda}_{10} + \frac{1}{\sigma^2_{v_{11}}}\mathbf{\Lambda}_{11} + \frac{1}{\sigma^2_{v_{12}}}\mathbf{\Lambda}_{12} \Bigg) \end{aligned} \tag{20}$$

where

$$\begin{aligned} & \mathbf{\Lambda}_1 = \widetilde{\mathbf{\Sigma}}_{s_1}, \quad \mathbf{\Lambda}_2 = \widetilde{\mathbf{\Sigma}}_{s_2}, \quad \mathbf{\Lambda}_3 = \widetilde{\mathbf{\Sigma}}_t \\ & \mathbf{\Lambda}_4 = \widetilde{\mathbf{\Sigma}}_{s_1} \otimes \mathbf{I}_{c_{s_2}-2}, \quad \mathbf{\Lambda}_5 = \mathbf{I}_{c_{s_1}-2} \otimes \widetilde{\mathbf{\Sigma}}_{s_2}, \quad \mathbf{\Lambda}_6 = \widetilde{\mathbf{\Sigma}}_{s_1} \otimes \mathbf{I}_2 \\ & \mathbf{\Lambda}_7 = \mathbf{I}_{c_{s_1}-q_{s_1}} \otimes \mathbf{I}_2, \quad \mathbf{\Lambda}_8 = \widetilde{\mathbf{\Sigma}}_{s_2} \otimes \mathbf{I}_{c_{t-2}} \quad \mathbf{\Lambda}_9 = \mathbf{I}_{c_{s_2}-2} \otimes \widetilde{\mathbf{\Sigma}}_t \\ & \mathbf{\Lambda}_{10} = \widetilde{\mathbf{\Sigma}}_{s_1} \otimes \mathbf{I}_{c_{s_2}-2} \otimes \mathbf{I}_{c_t-2}, \quad \mathbf{\Lambda}_{11} = \mathbf{I}_{c_{s_1}-2} \otimes \widetilde{\mathbf{\Sigma}}_{s_2} \otimes \mathbf{I}_{c_t-2}, \quad \mathbf{\Lambda}_{12} = \mathbf{I}_{c_{s_1}-2} \otimes \mathbf{I}_{c_{s_2}-2} \otimes \widetilde{\mathbf{\Sigma}}_t \end{aligned} \tag{21}$$

and $\widetilde{\mathbf{\Sigma}}$ matrices correspond to the non-zero eigenvectors resulting from the singular value decomposition of the penalty matrices.

2 Appendix B: Spatial distribution of aging in Italy

FIGURE B1
Sigma convergence

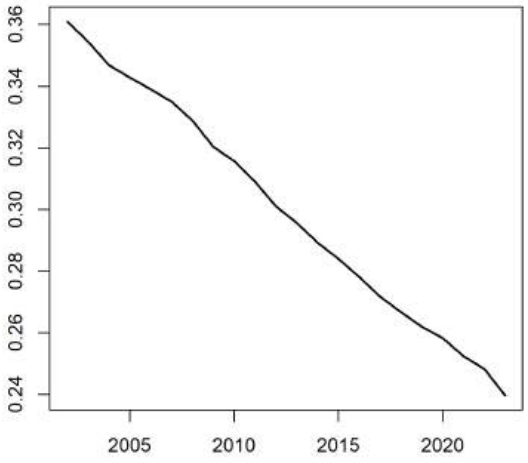

Source: personal elaboration on ISTAT data.

FIGURE B2
Local Moran I statistics

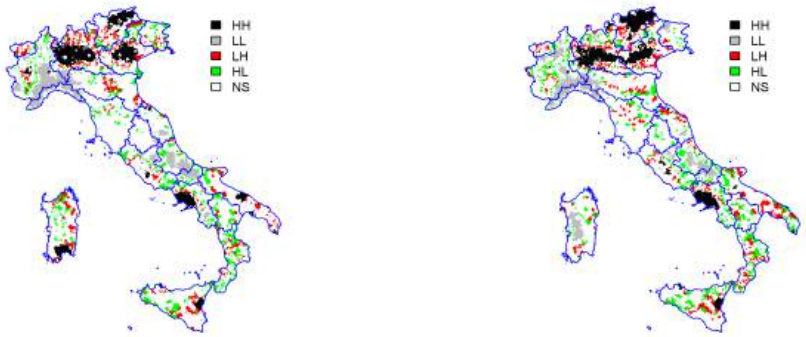

(a) 2002 (b) 2023

Source: personal elaboration on ISTAT data.

FIGURE B3
Local G statistics

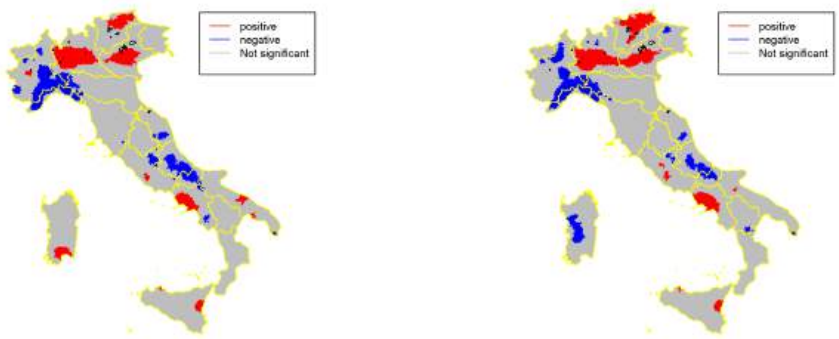

(a) 2002 (b) 2023

Source: Our elaboration on ISTAT data.

TABLE B1
Summary statistics for the PSR

	Min	First quartile	Median	Mean	Third quartile	Max
2002	56.600	255.600	324.700	340.500	409.100	1220.100
2003	61.540	253.740	320.710	335.770	402.800	1196.390
2004	57.890	253.040	317.930	332.870	396.420	1162.810
2005	59.260	249.690	312.740	326.740	387.490	1323.530
2006	56.000	246.600	308.100	320.900	379.200	1666.700
2007	55.260	245.680	305.490	317.260	374.010	1805.000
2008	56.340	247.140	305.280	316.850	371.520	2009.520
2009	53.450	247.640	304.480	315.340	369.090	1688.460
2010	54.100	247.400	302.500	313.000	365.400	1715.400
2011	54.240	248.380	301.880	311.820	362.970	1470.970
2012	57.140	243.750	295.710	304.590	353.000	1285.710
2013	52.500	240.000	289.800	298.300	344.900	1340.000
2014	47.500	235.400	283.100	291.100	335.600	1217.900
2015	44.740	230.980	276.780	284.230	326.840	1205.130
2016	47.890	227.290	271.910	278.590	318.670	1109.300
2017	50.000	224.600	266.800	273.700	312.400	985.100
2018	48.080	221.970	262.400	269.590	307.790	883.020
2019	53.190	219.710	258.700	265.170	302.490	852.850
2020	58.140	215.930	253.150	259.480	295.520	832.020
2021	62.070	212.740	248.670	254.810	289.950	820.000

TABLE B2
Summary statistics for the PSR

	Max-min	Inter-quartile range	Std. dev.	Coeff. of variation	Skewness	Kurtosis
2002	1163.448	153.487	122.857	0.361	1.069	5.810
2003	1134.848	149.059	118.999	0.354	1.022	5.536
2004	1104.911	143.374	115.439	0.347	1.002	5.406
2005	1264.270	137.804	112.017	0.343	1.063	6.024
2006	1610.667	132.655	108.768	0.339	1.193	8.111
2007	1749.737	128.330	106.285	0.335	1.287	9.973
2008	1953.186	124.372	104.183	0.329	1.462	13.921
2009	1635.013	121.450	101.036	0.320	1.244	9.562
2010	1661.286	117.967	98.844	0.316	1.308	10.559
2011	1416.730	114.595	96.391	0.309	1.167	8.175
2012	1228.571	109.248	91.737	0.301	1.075	7.080
2013	1287.500	104.921	88.217	0.296	1.109	7.832
2014	1170.449	100.222	84.209	0.289	1.088	7.417
2015	1160.391	95.861	80.741	0.284	1.081	7.633
2016	1061.415	91.383	77.496	0.278	1.061	7.290
2017	935.106	87.742	74.381	0.272	0.995	6.546
2018	834.942	85.828	71.923	0.267	0.943	6.131
2019	799.656	82.777	69.489	0.262	0.889	5.847
2020	773.881	79.595	67.024	0.258	0.865	5.879
2021	757.931	77.208	64.326	0.252	0.817	5.579

3 Appendix C: PSR change and its components

Figures C1-C7 provide a comprehensive view of the spatial distribution and temporal dynamics of changes in the Population Stability Ratio (PSR) and its components over two distinct subperiods: 2002-2011 and 2012-2023.

Panels a) and c) in Figure C1 illustrate the initial PSR values for each subperiod. Coastal areas in the South, along with Lombardy, Veneto, and the province of Bolzano, exhibit higher PSR values at the beginning of both periods, indicating a relatively younger and more stable population base. Panels b) and d) highlight the changes in PSR, with notable negative shifts observed particularly in regions with initially high PSR values. The second subperiod (2012-2023) shows a more severe decline in PSR, especially in southern Italy and some central coastal areas, reflecting intensified demographic challenges. In contrast, some municipalities in the Center and select regions in Sicily and Calabria exhibit either slightly positive or less negative PSR variations during the first subperiod (panel b), suggesting relative demographic resilience in these areas.

Panels a) and b) in Figure C2 depict the changes in PSR attributable to the old-age component. The patterns closely mirror the overall PSR trends, underscoring the significant impact of an aging population on PSR decline in both subperiods. Areas with higher initial PSR values experienced negative changes due to the increasing proportion of elderly individuals, starting from 2002-2011. This trend is exacerbated in 2012-2023, particularly in southern regions, where the rise in the elderly population has intensified the overall decline in PSR. Panels c) and d) focus on the contribution of the working-age population to PSR changes. During the first subperiod, the working-age component mitigated PSR decline, particularly in areas with higher initial PSR values. However, the second subperiod (2012-2023) reveals a general worsening of the situation, especially in southern Italy, indicating that the previously positive correlation between working-age population dynamics and initial PSR values has diminished.

Panels a) and b) in Figure C3 emphasize the positive influence of the cohort turnover component on PSR dynamics, particularly evident in southern Italy during 2002-2011. The presence of a robust cohort turnover and youthful population in these areas initially supported PSR stability. Nonetheless, by 2012-2023, the impact of cohort turnover diminished, reflecting an overall aging population and declining birth rates, with particularly pronounced effects in the South. Panels c) and d) illustrate the role of net migration, which had a beneficial effect on the working-age population during the first subperiod, especially in regions with initially high PSR values. Northern regions, Lazio, and some coastal southern areas experienced positive migration flows that counterbalanced aging trends. Conversely, the second period saw a predominance of negative migration balances in most southern areas, exacerbating the decline in the working-age population.

Panels a) and b) in Figure C4 demonstrate that internal migration patterns generally benefited northern areas, such as Lombardy and Emilia-Romagna, helping to alleviate PSR decline. In contrast, the South experienced a negative internal migration balance, a trend that intensified in 2012-2023. Panels c) and d) reveal that international migration has significantly impacted northern Italy, with a noticeable positive migration balance in the South during the second period partially offsetting the effects of aging and internal outmigration.

Panels a) and b) in Figure C5 highlight the persistent outflow of Italian citizens from southern to northern areas. Coastal southern regions showed a positive migration balance in the first subperiod, but the second subperiod saw a marked deterioration, particularly in Apulia, Calabria, and some northern areas like Bolzano. Panels c) and d) illustrate the increasing contribution of foreign migration to working-age population growth, especially in northern and central Italy. This positive effect of foreign migration became more significant in 2012-2023, helping to mitigate demographic decline in the South.

Panels a) and b) in Figure C6 underscore the trend of Italians moving towards economically vibrant regions, such as Rome and northern industrial centers, with a worsening internal migration balance in the South during 2012-2023. Panels c) and d) confirm that foreign internal migrants are increasingly settling in economically advantageous areas, particularly in the North. This trend is more pronounced in the second period, with foreign migrants increasingly favoring northern regions from southern areas.

Panels a) and b) in Figure C7 highlight the significant variation in Italian international migration during the first subperiod, with negative balances observed in Bolzano and several southern areas. This trend worsens in the second subperiod (2012-2023), reflecting a generalized negative balance across most regions. Panels c) and d) emphasize the crucial role of foreign international migration in offsetting population decline, particularly in northern Italy. The impact of foreign immigration becomes increasingly substantial in the second period, underscoring the growing reliance on international migrants to maintain demographic stability, even in the South.

FIGURE C1
PSR Initial Conditions and PSR Change

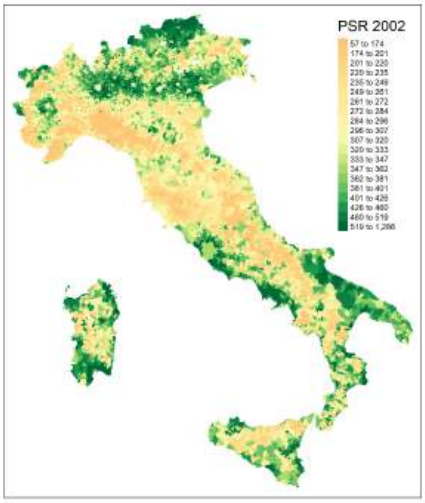

(a) PSR 2002

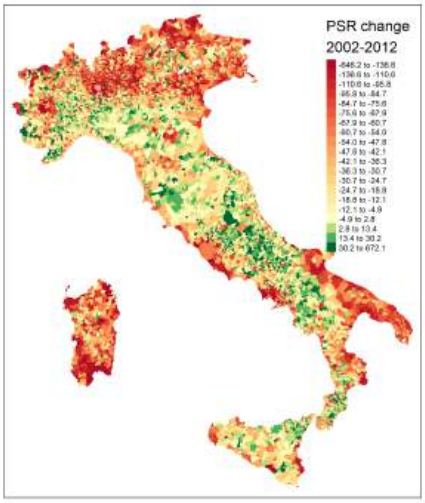

(b) PSR Change 2002-2012

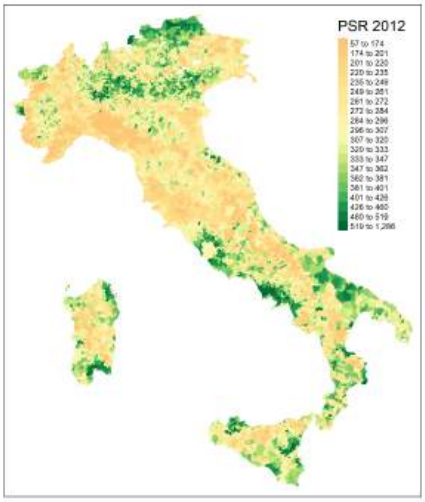

(c) PSR 2012

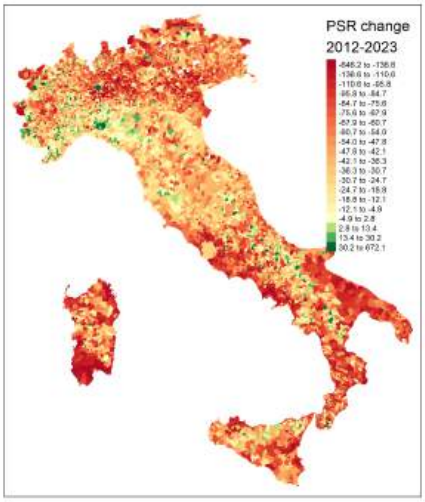

(d) PSR Change 2012-2023

Source: Our elaboration on ISTAT data.

FIGURE C2
Old-Age and Working-Age Components

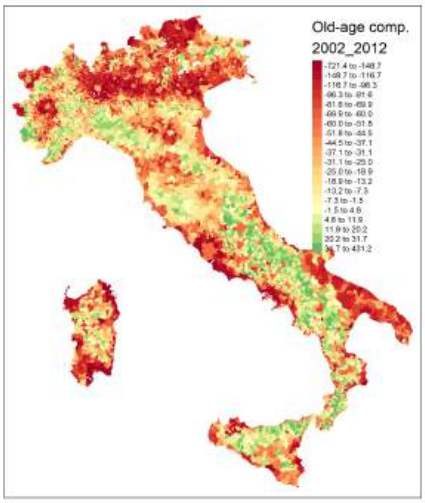

(a) Old Age 2002-2012

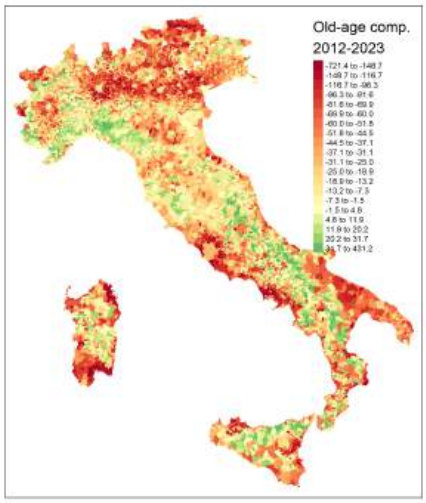

(b) Old Age 2012-2023

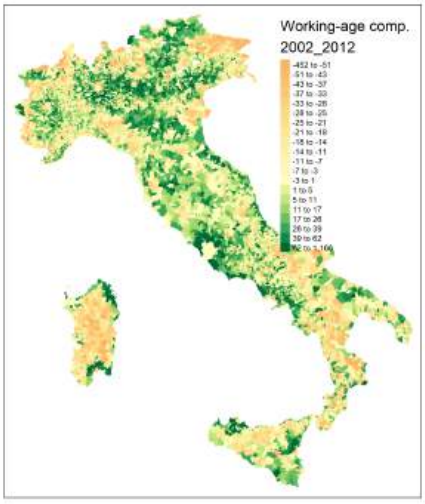

(c) Working Age 2002-2012

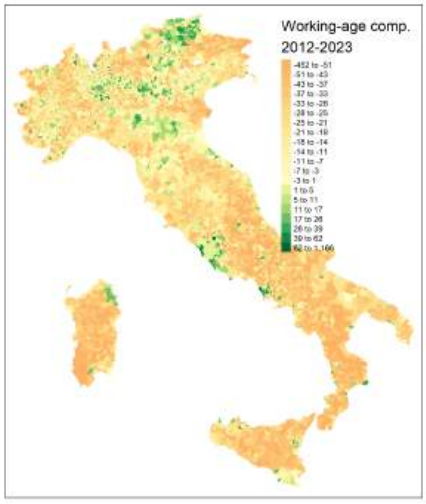

(d) Working Age 2012-2023

Source: Our elaboration on ISTAT data.

FIGURE C3
Cohort Turnover and Migration Components

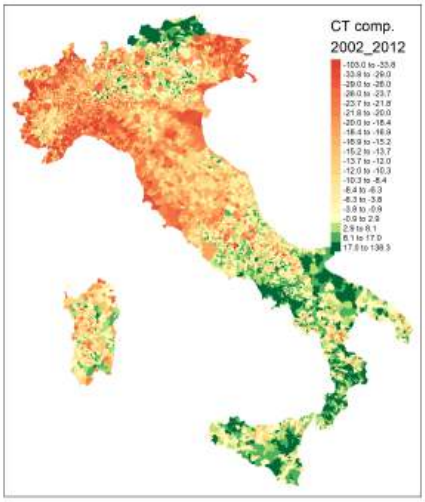

(a) Cohort Turnover 2002-2012

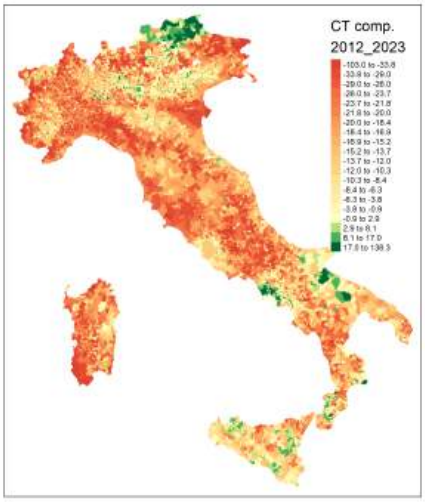

(b) Cohort Turnover 2012-2023

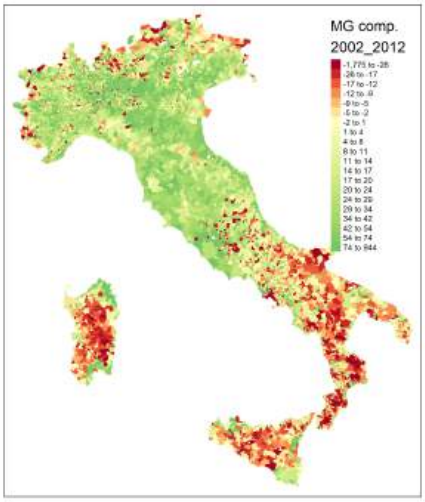

(c) Migration 2002-2011

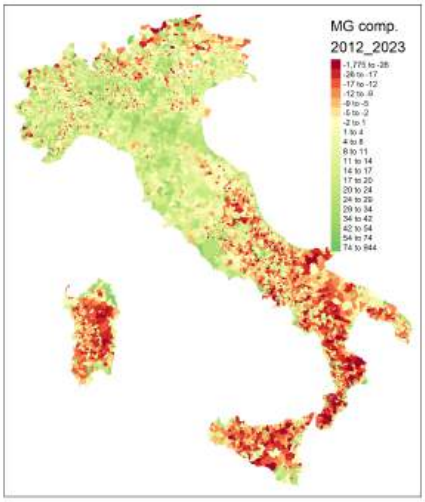

(d) Migration 2012-2023

Source: Our elaboration on ISTAT data.

FIGURE C4
Internal and International Migration Components

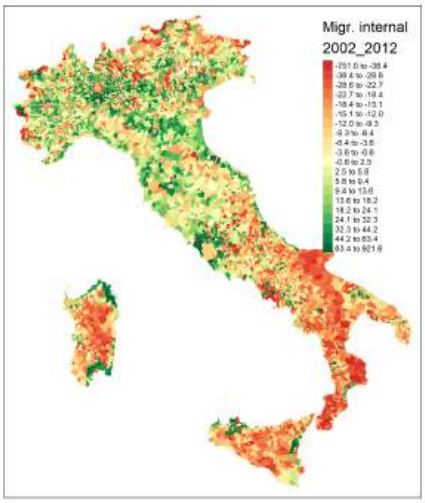

(a) Internal Migration 2002-2012

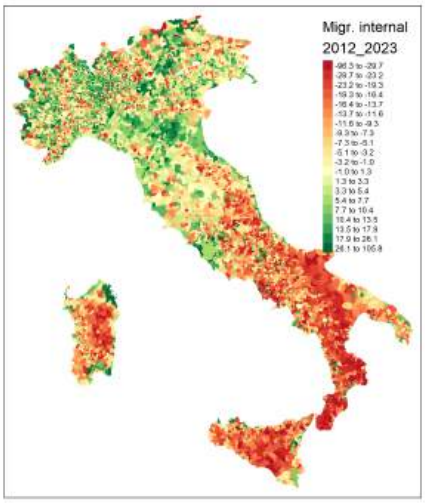

(b) Internal Migration 2012-2023

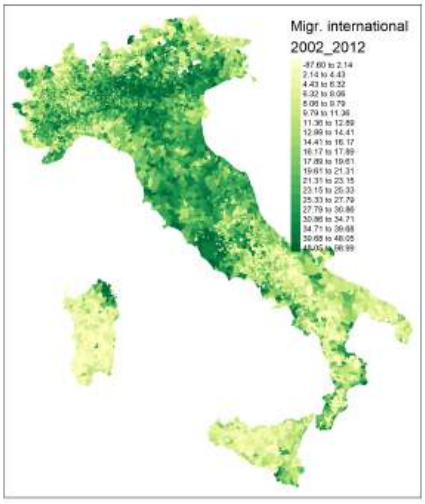

(c) International Migration 2002-2012

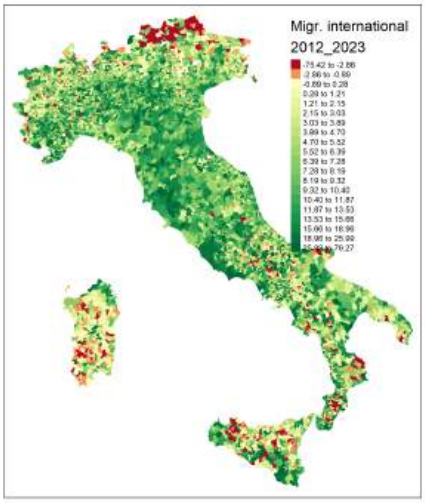

(d) International Migration 2012-2023

Source: Our elaboration on ISTAT data.

FIGURE C5
Italian and Foreign Migration Components

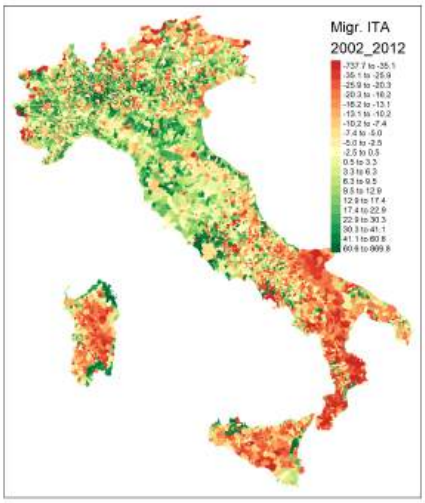

(a) Italian Migration 2002-2012

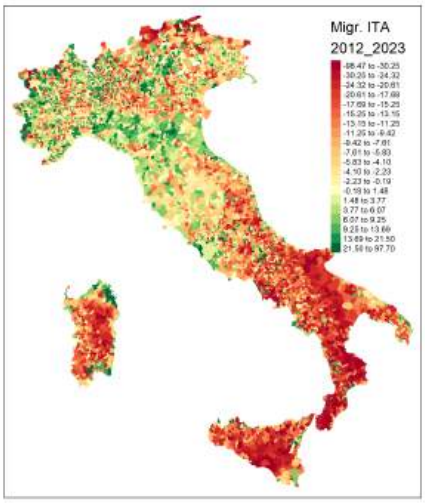

(b) Italian Migration 2012-2023

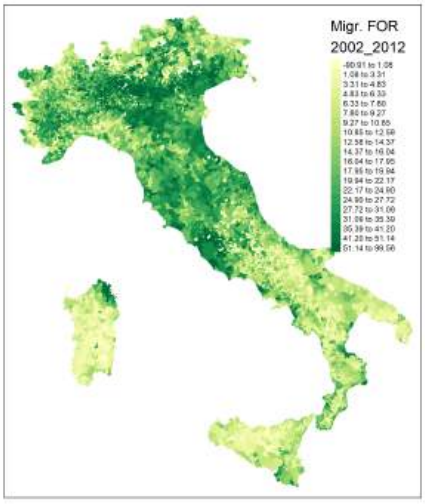

(c) Foreign Migration 2002-2012

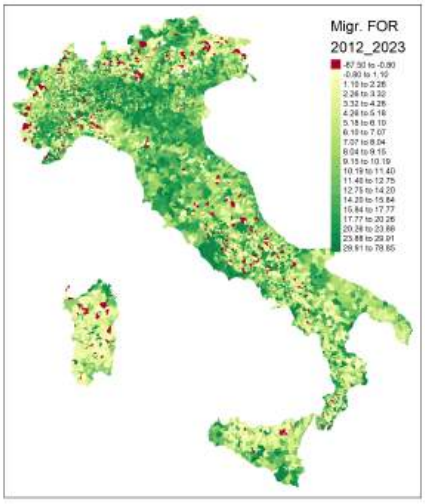

(d) Foreign Migration 2012-2023

Source: Our elaboration on ISTAT data.

FIGURE C6
Italian and Foreign Internal Migration Components

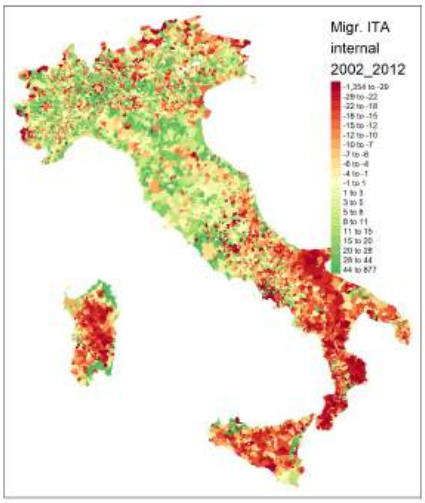

(a) Italian Internal Migration 2002-2012

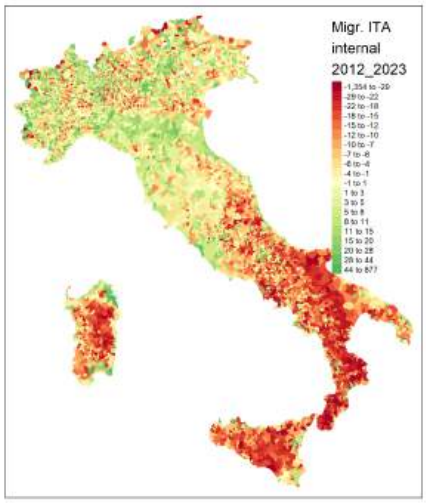

(b) Italian Internal Migration 2012-2023

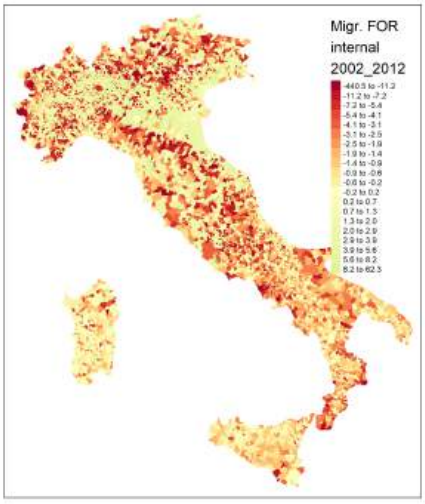

(c) Foreign Internal Migration 2002-2012

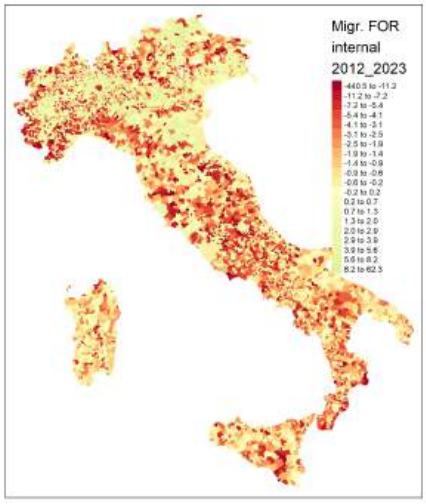

(d) Foreign Internal Migration 2012-2023

Source: Our elaboration on ISTAT data.

FIGURE C7
Italian and Foreign International Migration Components

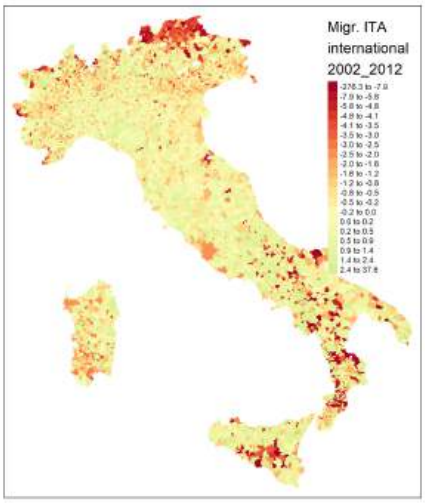

(a) Italian International Migration 2002-2012

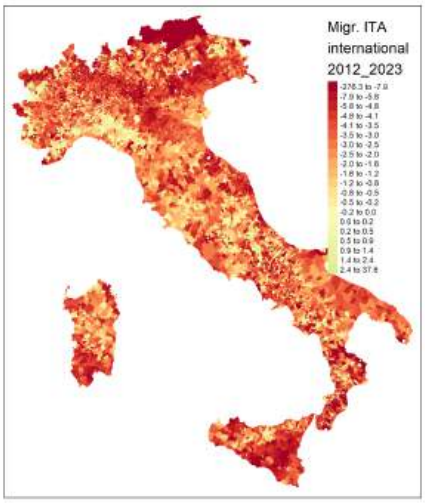

(b) Italian International Migration 2012-2023

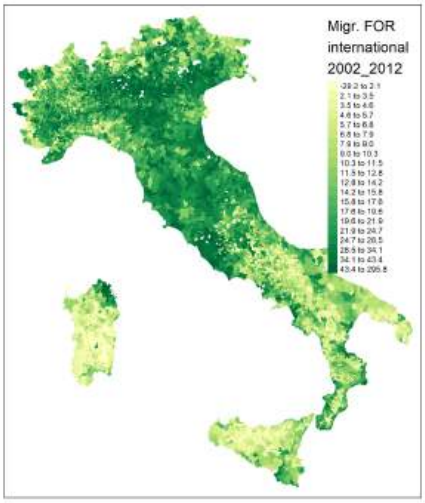

(c) Foreign International Migration 2002-2012

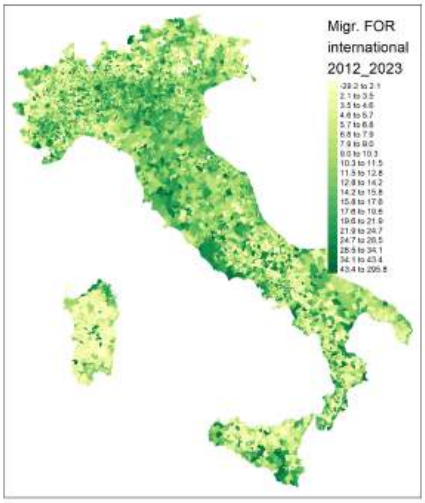

(d) Foreign International Migration 2012-2023

Source: Our elaboration on ISTAT data.

References

BASILE, R., M. DURBÁN, R. MÍNGUEZ, J. M. MONTERO, AND J. MUR (2014): "Modeling regional economic dynamics: spatial dependence, spatial heterogeneity and nonlinearities," *Journal of Economic Dynamics and Control*, 48, 229–245.

DE BOOR, C. (1977): "Package for calculating with B-splines," *Journal of Numerical Analysis*, 14, 441–472.

EILERS, P., I. CURRIE, AND M. DURBÁN (2006): "Fast and compact smoothing on large multidimensional grids," *Computational Statistics and Data Analysis*, 50(1), 61–76.

EILERS, P., AND B. MARX (1996): "Flexible Smoothing with B-Splines and Penalties," *Statistical Science*, 11, 89–121.

LEE, D. (2010): "Smoothing mixed models for spatial and spatio-temporal data," Ph.D. thesis, University Carlos-III.

LEE, D., AND M. DURBÁN (2011): "P-Spline ANOVA Type Interaction Models for Spatio-Temporal Smoothing," *Statistical Modelling*, 11, 49–69.

MÍNGUEZ, R., R. BASILE, AND M. DURBÁN (2020): "An alternative semiparametric model for spatial panel data," *Statistical Methods & Applications*, 29(4), 669–708.

WOOD, S. (2010): "More advanced use of mgcv," *Course notes available from: http://people. bath. ac. uk/sw283/mgcv/tampere/mgcv-advanced. pdf (accessed November 2013)*.